# NSM FRP STRIPS SHEAR STRENGTH CONTRIBUTION TO A RC BEAM: A DESIGN PROCEDURE

Vincenzo Bianco, Giorgio Monti and J.A.O. Barros

**Synopsis:** This paper presents a closed-form procedure to evaluate the shear strength contribution provided to a Reinforced Concrete (RC) beam by a system of Near Surface Mounted (NSM) Fiber Reinforced Polymer (FRP) strips. This procedure is based on the evaluation of: a) the *constitutive law* of the average-available-bond-length NSM FRP strip effectively crossing the shear crack and b) the *maximum effective capacity* it can attain during the loading process of the strengthened beam. Due to complex phenomena, such as: a) interaction between forces transferred through bond to the surrounding concrete and concrete fracture, and b) interaction among adjacent strips, the NSM FRP strip constitutive law is largely different than the linear elastic one characterizing the FRP behavior in tension. Once the constitutive law of the average-available-bond-length NSM strip is reliably known, its maximum effective capacity can be determined by imposing a coherent *kinematic mechanism*. The self-contained and ready-to-implement set of analytical equations and logical operations is presented along with the main underlying physical-mechanical principles and assumptions. The formulation proposed is appraised against some of the most recent experimental results and its predictions are also compared with those obtained by a recently developed more sophisticated model.

**Keywords**: Concrete Fracture; Debonding; Design; FRP; NSM; Shear Strengthening; Tensile Rupture.

**Vincenzo Bianco** is a Post Doc at the Department of Structural Engineering and Geotechnics of the Sapienza University of Rome, Italy. He received his PhD from the Sapienza University of Rome. His research interests include seismic assessment and retrofit of existing structures, mechanical modeling and use of composite materials for structural rehabilitation.

**Giorgio Monti** is a Full Professor at the Department of Structural Engineering and Geotechnics of the Sapienza University of Rome, Italy. He received is MSc from the University of Berkley, California, and his PhD from the Sapienza University of Rome. His Research interests span from reliability to the assessment and retrofitting of existing structures in seismic zones.

**Joaquim Barros** is an Associate Professor with aggregation and Director of the Laboratory of the Structural Group of the Department of Civil Engineering, University of Minho at Guimarães, Portugal. He received his MSc and PhD from the University of Porto, Portugal. He is a member of ACI Committees 440 and 544, and fib TG 8.3 and 9.3. His research interests include structural strengthening, composite materials, fiber reinforced concrete and finite element method.

## INTRODUCTION

Shear strengthening of RC beams by NSM technique consists of bonding FRP strips by a powerful structural adhesive into thin shallow slits cut onto the concrete cover of the beam web lateral faces. A comprehensive three-dimensional mechanical model to predict the NSM FRP strips shear strength contribution to a RC beam was recently developed (Bianco 2008, Bianco *et al.* 2009a-b and 2010). Despite its consistency with experimental recordings, that model turned out to be somehow cumbersome to be easily implemented and accepted by professional structural engineers. The aim of the present work is to develop a simpler computational procedure that has to be: a) *mechanically-based* and b) *simple to implement*. As to the first point, it has to fulfill equilibrium, kinematic compatibility and constitutive laws. As to the second point, it has to be a design tool easy to apply. For this purpose, a reasonable compromise between accuracy of prediction and computational demand has to be achieved. Excessively simplified assumptions, which would provide too roughly conservative estimates of the shear strength contribution provided by a system of NSM FRPs, should be avoided since they could lead to uneconomical design solutions, discouraging application, further improvement and spreading of the technique. A relatively simple model can be derived from the more sophisticated one by introducing the following simplifications (Bianco 2008): 1) a bi-linear rigid-softening local bond stress-slip diagram is adopted instead of a multi-linear diagram, 2) concrete fracture surface is assumed as semi-pyramidal instead of semi-conical, 3) attention is focused on the average-available-bond-length NSM FRP strip glued on the relevant prism of surrounding concrete, 4) determining the constitutive law of the average-available-bond-length NSM strip, along the approach followed for Externally Bonded Reinforcement (EBR) by Monti *et al.* (2003), and 5) determining the maximum effective capacity attainable by the average-available-bond-length NSM strip placed along the CDC, imposing a coherent kinematic mechanism (*e.g.* Monti *et al.* 2004, Monti and Liotta 2007). The main features of the resulting modeling strategy are reported hereafter.

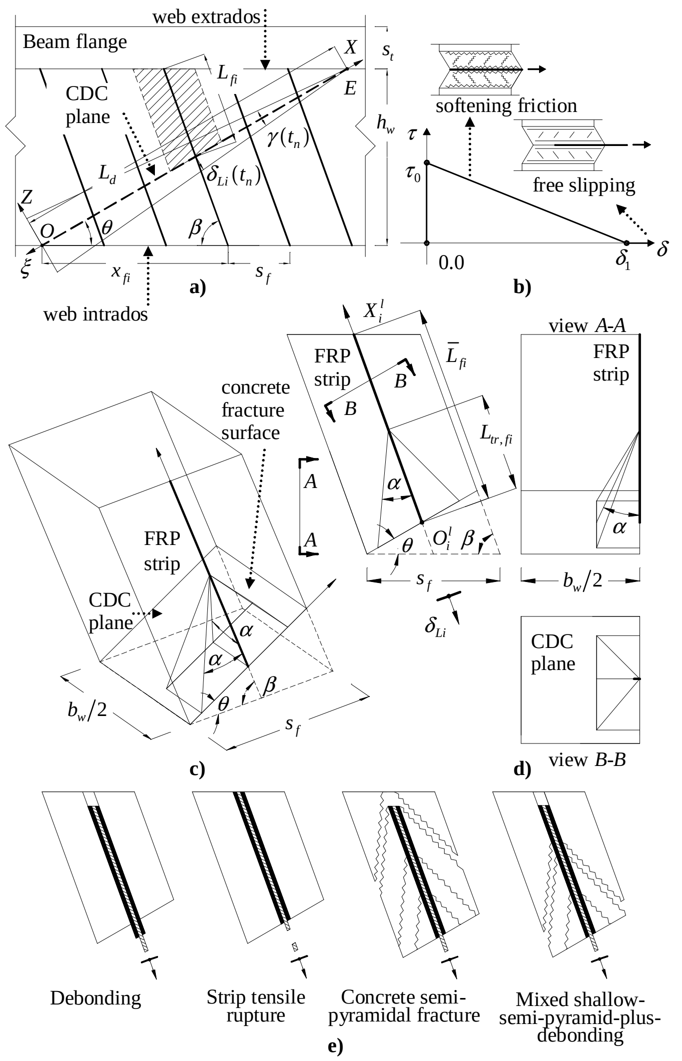


**Figure 1** — Main physical-mechanical features of the calculation procedure: a) average-available-bond-length NSM strip and relevant prism of surrounding concrete, b) adopted local bond stress-slip relationship, c) NSM strip confined to the corresponding concrete prism of surrounding concrete and semi-pyramidal fracture surface, d) sections of the concrete prism.

During the loading process of a RC beam subject to shear, when concrete average tensile strength $f_{ctm}$ is attained at the web intrados (Fig. 1), some shear cracks originate therein and successively progress towards the web extrados. Those cracks can be thought as a single Critical Diagonal Crack (CDC) inclined of an angle $\theta$ with respect to the beam longitudinal axis (Fig. 1a). The CDC can be represented by an inclined plane dividing the web into two portions sewn together by the crossing strips (Fig. 1a). At load step $t_1$, the two web parts, separated by the CDC, start moving apart by pivoting around the crack end whose trace, on the web face, is point *E* in Fig. 1a. From that step on, by increasing the applied load, the CDC opening angle $\gamma(t_n)$ progressively widens (Fig. 1a). The strips crossing the CDC oppose its widening by anchoring to the surrounding concrete to which they transfer, by bond, the force originating at their intersection with the CDC, $O_i^l$, as a result of the imposed end slip $\delta_{Li}[\gamma(t_n)]$. The capacity of each strip is provided by its available bond length $L_{fi}$ that is the shorter between the two parts into which the crack divides its actual length $L_f$ (Fig. 1a). Bond is the mechanism through which stresses are transferred to the surrounding concrete (Yuan *et al.* 2004, Mohammed Ali *et al.* 2006 and 2007, Bianco *et al.* 2007). The local bond stress-slip relationship $\tau(\delta)$, comprehensively simulating the mechanical phenomena occurring at 1) the strip-adhesive interface, 2) within the adhesive layer and at 3) the adhesive-concrete interface, can be represented, in a simplified way, by a bi-linear curve (Fig. 1b). The subsequent phases undergone by bond during the loading process, representing the physical phenomena occurring in sequence within the adhesive layer by increasing the imposed end slip, are: "rigid", "softening friction" and "free slipping" (Fig. 1b) (Bianco 2008).

The constitutive law $V_{fi}\left(L_{Rfi};\delta_{Li}\right)$ of an NSM FRP strip, *i.e.* the force transmissible by a strip with resisting bond length $L_{Rfi}$ as function of the imposed end slip $\delta_{Li}$, can be determined by analyzing the behavior of the simple structural element composed of the NSM FRP strip within a concrete prism (Fig. 1a,c-d) whose transversal dimensions are limited by the spacing $s_f$ between adjacent strips and half of the web cross section width $b_w/2$. In this way, the problem of interaction between adjacent strips (*e.g.*: Dias and Barros 2008, Rizzo and De Lorenzis 2009) is taken into account in a simplified way, *i.e.*, by limiting the concrete volume into which subsequent fractures can form, to the amount of surrounding concrete pertaining to the single strip in dependence of $s_f$ and $b_w$. Moreover, even though here neglected, the interaction with existing stirrups may be also accounted for by limiting the transversal dimension of the concrete prism to a certain ratio of $b_w/2$, since the larger the amount of stirrups, the shallower concrete fracture is expected to be (Bianco *et. al* 2006) even if, in this respect, further research is necessary.

In particular, in the present work, attention is focused on the system composed of the strip with the average value of available bond length glued on the pertaining prism of surrounding concrete (Fig. 1c-d).

The failure modes of an NSM FRP strip subject to an imposed end slip comprise, depending on the relative mechanical and geometrical properties of the materials involved: debonding, tensile rupture of the strip, concrete semi-pyramidal tensile fracture and a mixed shallow-semi-pyramid-plus-debonding failure mode (Fig. 1e). The term *debonding* is adopted to designate loss of bond due to damage initiation and propagation within the adhesive layer and at the FRP strip-adhesive and adhesive-concrete interfaces, so that the strip pulling out results (Fig. 1e). When principal tensile stresses transferred to the surrounding concrete attain its tensile strength, concrete fractures along a surface, envelope of the compression isostatics, whose shape can be conveniently assumed as a semi-pyramid with principal generatrices inclined of an angle $\alpha$ with respect to the strip longitudinal axis (Fig. 1c-d). Increasing the imposed end slip can result in subsequent semi-pyramidal and coaxial fracture surfaces in the concrete surrounding the NSM strip. These progressively reduce the resisting bond length $L_{Rfi}$ that is the portion of the initial available bond length $L_{fi}$ still bonded to concrete. Those subsequent fractures can either progress up to the free end, resulting in a *concrete semi-pyramidal failure*, or stop progressing midway between loaded and free end, resulting in a *mixed-shallow-semi-pyramid-plus-debonding* failure (Fig. 1e). Moreover, regardless of an initial concrete fracture, the strip can *rupture* (Fig. 1e).

The formulation obtained by this strategy is presented in the following sections along with the main mechanical bases.

## RESEARCH SIGNIFICANCE

A calculation procedure was developed to evaluate the NSM FRP strips shear strength contribution to a RC beam. The equations and the logical operations necessary to implement the proposed procedure are presented along with the theoretical bases form which they originate.

## CALCULATION PROCEDURE

The input parameters include (Figs. 1-2): beam cross-section web's depth $h_w$ and width $b_w$; inclination angle of both CDC and strips with respect to the beam longitudinal axis, $\theta$ and $\beta$, respectively; strips spacing measured along the beam axis $s_f$; angle $\alpha$ between axis and principal generatrices of the semi-pyramidal fracture surface (Fig. 1c-d); concrete average compressive strength $f_{cm}$; strips tensile strength $f_{fu}$ and Young's modulus $E_f$; thickness $a_f$ and width $b_f$ of the strip cross-section; increment $\dot{\delta}_{Li}$ of the imposed end slip; values of bond stress $\tau_0$ and slip $\delta_1$ defining the adopted local bond stress-slip relationship (Fig. 1b):

$$\tau(\delta) = \begin{cases} \tau_0 \left(1 - \dfrac{\delta}{\delta_1}\right) & 0 < \delta \le \delta_1 \\ 0 & \delta > \delta_1 \end{cases} \qquad (1)$$

The geometrical configuration is adopted in which the minimum integer number $N^l_{f,\text{int}}$ of strips cross the CDC with the first one placed at a distance equal to $s_f$ from the crack origin (Fig. 1a). This configuration corresponds to the minimum of the sum of all the available bond lengths $L_{fi}$. $N^l_{f,\text{int}}$ is obtained by rounding off the real number to the lowest integer, as follows:

$$N^l_{f,\text{int}} = \text{round off}\left[h_w \cdot \frac{(\cot\theta + \cot\beta)}{s_f}\right] \qquad (2)$$

and the average available bond length $\bar{L}_{fi}$ is obtained by:

$$\bar{L}_{fi} = \frac{1}{N^l_{f,\text{int}}} \cdot \sum_{i=1}^{N^l_{f,\text{int}}} L_{fi} \qquad (3)$$

with:

$$L_{fi}=\begin{cases} i\cdot s_f\cdot\dfrac{\sin\theta}{\sin(\theta+\beta)} & \text{for}\quad x_{fi}<\dfrac{h_w}{2}\cdot(\cot\theta+\cot\beta)\\ L_f-i\cdot s_f\cdot\dfrac{\sin\theta}{\sin(\theta+\beta)} & \text{for}\quad x_{fi}\geq\dfrac{h_w}{2}\cdot(\cot\theta+\cot\beta)\end{cases} \tag{4}$$

and:

$$x_{fi}=i\cdot s_f \tag{5}$$

After having defined the geometrical characteristics of the simple structural system composed of the average-available-bond-length strip within the relevant prism of surrounding concrete, it is necessary to determine its constitutive law $V_{fi}\left(\bar{L}_{fi};\delta_{Li}\right)$ and the corresponding maximum effective capacity $V_{fi}^{\max}$, as explained hereafter. Once $V_{fi}^{\max}$ has been obtained, the actual $V_f$ and design $V_{fd}$ values of the NSM shear strength contribution can be obtained by Eq. (36).

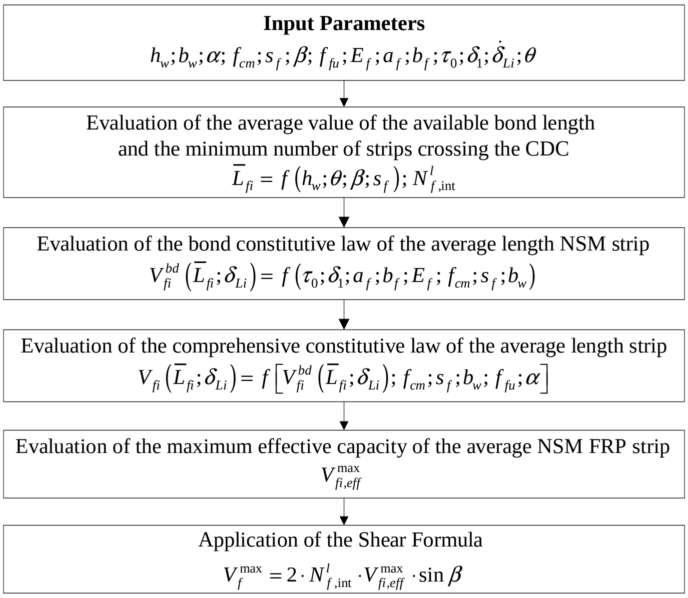


**Figure 2 —** Calculation procedure: main algorithm.

## CONSTITUTIVE LAW OF A SINGLE NSM FRP STRIP

The simple structural system composed of a single strip, the adhesive and the surrounding concrete, undergoes changes during the loading process since, each time concrete fractures, the resisting bond length reduces accordingly. In particular, the different features assumed by that system throughout the loading process are function not only of the load step $t_n$, but also of the iteration $q_m$ in correspondence of $t_n$ (Bianco 2008). In fact, for each $t_n$, that system undergoes modifications up to reaching the equilibrium configuration $q_e$. Whenever concrete fractures, the mechanism of force transfer to the surrounding concrete leaps forward towards the strip's free end. In general, in correspondence of each leap, the overall transfer length $L_{tr,fi}\left(L_{Rfi};\delta_{Li}\right)$ increases and the resisting bond length decreases (Fig. 1c-d). Thus, in general, at each leap, concrete tensile fracture capacity increases and at the same time the bond-transferred force decreases, until equilibrium is attained. In this scenario, in order to determine the comprehensive constitutive law $V_{fi}\left(\bar{L}_{fi};\delta_{Li}\right)$ of the average-available-bond-length NSM FRP strip bonded to the relevant prism of surrounding concrete, it is necessary to carry out an incremental procedure that simulates the imposed end slip $\delta_{Li}(t_n)$ and to check, at each $t_n$, either if concrete is capable of carrying the bond-transferred stresses without undergoing fracture, or if a concrete fracture occurs and the system has to be modified accordingly.

**Bond-based constitutive law**

The bond behaviour of an NSM FRP strip subject to an increasing imposed end slip can be modelled by fulfilling equilibrium, kinematic compatibility and constitutive laws of both adhered materials (concrete and FRP) and local bond between themselves (Bianco 2008). In this way, it is possible to obtain closed-form analytical equations for both the bond-based constitutive law $V_{fi}^{bd}\left(L_{Rfi};\delta_{Li}\right)$ of a single strip and the corresponding bond transfer length $L_{tr,fi}^{bd}\left(L_{Rfi};\delta_{Li}\right)$. The latter two quantities, $V_{fi}^{bd}\left(L_{Rfi};\delta_{Li}\right)$ and $L_{tr,fi}^{bd}\left(L_{Rfi};\delta_{Li}\right)$, represent: the force a strip of resisting bond length $L_{Rfi}$ can transfer by bond, as function of $\delta_{Li}$, and the corresponding amount of $L_{Rfi}$ along which bond is mobilized, respectively. The analytical equations of $L_{tr,fi}^{bd}\left(L_{Rfi};\delta_{Li}\right)$ and $V_{fi}^{bd}\left(L_{Rfi};\delta_{Li}\right)$, are presented below and plotted in Fig. 3. Those analytical equations envisage, for a given $L_{Rfi}$, three phases, whose limits ($\delta_{L1};\delta_{L2};\delta_{L3}$) are function of the value assumed by $L_{Rfi}$ with respect to the effective bond length $L_{tr1}$ that is the value of resisting bond length beyond which any further increase of length does not produce any further increase of the maximum force transmissible by bond. The bond transfer length is as follows:

$$
\begin{array}{ll}
L_{tr,fi}^{bd}\left(L_{Rfi};\delta_{Li}\right)=L_{tr}^{sf}\left(\delta_{Li}\right)= & \\
\dfrac{1}{\lambda}\cdot\arccos\left(1-\dfrac{\lambda^2}{\tau_0\cdot J_1}\cdot\delta_{Li}\right) & 0.0\le\delta_{Li}\le\delta_{L1}\left(L_{Rfi}\right) \\
\begin{cases} L_{tr,fi}^{bd}\left(L_{Rfi}<L_{tr1};\delta_{Li}\right)=L_{Rfi} \\ L_{tr,fi}^{bd}\left(L_{Rfi}\ge L_{tr1};\delta_{Li}\right)=L_{tr1}+L_{tr}^{fs}\left(\delta_{Li}\right) \end{cases} & \delta_{L1}\left(L_{Rfi}\right)<\delta_{Li}\le\delta_{L2}\left(L_{Rfi}\right) \\
L_{tr,fi}^{bd}\left(L_{Rfi};\delta_{Li}\right)=L_{Rfi} & \delta_{L2}\left(L_{Rfi}\right)<\delta_{Li}\le\delta_{L3}\left(L_{Rfi}\right) \\
L_{tr,fi}^{bd}\left(L_{Rfi};\delta_{Li}\right)=0.0 & \delta_{Li}>\delta_{L3}\left(L_{Rfi}\right)
\end{array}
\tag{6}
$$

and the bond-based constitutive law:

$$
\begin{array}{ll}
V_{fi}^{bd}\left(L_{Rfi};\delta_{Li}\right)=L_p\cdot J_3\cdot\lambda\cdot & \\
\cdot\left\{C_1^{sf}\cdot\left[\cos\left(\lambda\cdot L_{tr}^{sf}\left(\delta_{Li}\right)\right)-1\right]-C_2^{sf}\cdot\sin\left(\lambda\cdot L_{tr}^{sf}\left(\delta_{Li}\right)\right)\right\} & 0.0\le\delta_{Li}\le\delta_{L1}\left(L_{Rfi}\right) \\
\begin{cases} V_{fi}^{bd}\left(L_{Rfi}<L_{tr1};\delta_{Li}\right)=L_p\cdot J_3\cdot\lambda\cdot \\ \cdot\left[C_1^{sf}\cdot\cos\left(\lambda\cdot x^{sf}\right)-C_2^{sf}\cdot\sin\left(\lambda\cdot x^{sf}\right)\right]_{L_{tr}^{sf}\left(\delta_{Li}\right)-L_{Rfi}}^{L_{tr}^{sf}\left(\delta_{Li}\right)} \\ V_{fi}^{bd}\left(L_{Rfi}\ge L_{tr1};\delta_{Li}\right)=V_{f1}^{bd} \end{cases} & \delta_{L1}\left(L_{Rfi}\right)<\delta_{Li}\le\delta_{L2}\left(L_{Rfi}\right)
\end{array}
\tag{7}
$$

$$V_{fi}^{bd}\left(L_{Rfi};\delta_{Li}\right)=L_p\cdot J_3\cdot\lambda\cdot\left[C_1^{sf}\cdot\cos\left(\lambda\cdot x^{sf}\right)-C_2^{sf}\cdot\sin\left(\lambda\cdot x^{sf}\right)\right]_{L_{tr1}+L_{tr}^{fs}(\delta_{Li})-L_{Rfi}}^{L_{tr1}} \qquad \delta_{L2}\left(L_{Rfi}\right)<\delta_{Li}\leq\delta_{L3}\left(L_{Rfi}\right)$$

$$V_{fi}^{bd}\left(L_{Rfi};\delta_{Li}\right)=0.0 \qquad \delta_{Li}>\delta_{L3}\left(L_{Rfi}\right)$$

where:

$$L_p=2\cdot b_f+a_f \tag{8}$$

is the effective perimeter of the strip cross-section, and:

$$\frac{1}{\lambda^2}=\frac{\delta_1}{\tau_0\cdot J_1};J_1=\frac{L_p}{A_f}\cdot\left[\frac{1}{E_f}+\frac{A_f}{A_c\cdot E_c}\right];J_2=\frac{E_f\cdot E_c\cdot A_c}{E_c\cdot A_c+E_f\cdot A_f}$$
$$J_3=\frac{E_f\cdot A_f\cdot E_c\cdot A_c}{L_p\cdot\left(A_c\cdot E_c+A_f\cdot E_f\right)};C_1^{sf}=\delta_1-\frac{\tau_0\cdot J_1}{\lambda^2};C_2^{sf}=-\frac{\tau_0\cdot J_1}{\lambda^2} \tag{9}$$

are bond-modeling constants (Bianco 2008, Bianco *et al.* 2009b), with $A_f=a_f\cdot b_f$ and $A_c=s_f\cdot b_w/2$ the cross-section of the strip and the concrete prism, respectively. Moreover, the effective bond length $L_{tr1}$ and the corresponding maximum bond force $V_{f1}^{bd}$ are given by:

$$L_{tr1}=\frac{\pi}{2\cdot\lambda};V_{f1}^{bd}=L_p\cdot J_3\cdot\lambda\cdot\left[\frac{2\cdot\tau_0\cdot J_1}{\lambda^2}-\delta_1\right] \tag{10}$$

The value of resisting bond length undergoing softening friction, as function of the imposed end slip is given by:

$$L_{tr}^{sf}(\delta_{Li})=\frac{1}{\lambda}\cdot\arccos\left[1-\frac{\lambda^2}{\tau_0\cdot J_1}\cdot\delta_{Li}\right] \tag{11}$$

and the value of resisting bond length undergoing free slipping:

$$L_{tr}^{fs}(\delta_{Li})=\frac{A_f\cdot J_2\cdot(\delta_{Li}-\delta_1)}{V_{f1}^{bd}} \tag{12}$$

The resisting bond length-dependent values of imposed end slip defining the extremities of the three bond phases, are given by (Fig. 3):

$$\delta_{L1}\left(L_{Rfi}\right)=\begin{cases}C_1^{sf}\cdot\sin\left(\lambda\cdot L_{Rfi}\right)+C_2^{sf}\cdot\cos\left(\lambda\cdot L_{Rfi}\right)+\dfrac{\tau_0\cdot J_1}{\lambda^2} & \text{for } L_{Rfi}<L_{tr1}\\ \delta_1 & \text{for } L_{Rfi}\geq L_{tr1}\end{cases} \tag{13}$$

$$\delta_{L2}\left(L_{Rfi}\right)=\begin{cases}\delta_1 & \text{for } L_{Rfi}<L_{tr1}\\ \delta_1+\dfrac{V_{f1}^{bd}}{A_f\cdot J_2}\cdot\left(L_{Rfi}-L_{tr1}\right) & \text{for } L_{Rfi}\geq L_{tr1}\end{cases} \tag{14}$$

$$\delta_{L3}\left(L_{Rfi}\right)=\delta_1+\frac{L_{Rfi}\cdot V_{f1}^{bd}}{A_f\cdot J_2} \tag{15}$$

**Concrete tensile fracture capacity**

The concrete tensile fracture capacity $V_{fi}^{cf}\left(L_{tr,fi}\right)$ is obtained by spreading the concrete average tensile strength $f_{ctm}$ over the semi-pyramidal surface (Fig. 1c-d) of height equal to the total transfer length $L_{tr,fi}$, orthogonally to it in each point. By integrating one obtains:

$$V_{fi}^{cf}\left(L_{tr,fi}\right)= f_{ctm}\cdot\min\left\{L_{tr,fi}\cdot\tan\alpha;\frac{b_w}{2}\right\}\cdot\sin\left(\theta+\beta\right)\cdot \\ \cdot\left(\min\left\{\frac{s_f\cdot\sin\beta}{2\cdot\sin\left(\theta+\beta\right)};\frac{L_{tr,fi}\cdot\sin\alpha}{\sin\left(\theta+\beta+\alpha\right)}\right\}+\min\left\{\frac{s_f\cdot\sin\beta}{2\cdot\sin\left(\theta+\beta\right)};\frac{L_{tr,fi}\cdot\sin\alpha}{\sin\left(\theta+\beta-\alpha\right)}\right\}\right) \tag{16}$$

where $f_{ctm}$ can be determined from the average compressive strength. The total transfer length is evaluated as reported in next Eq. (17).

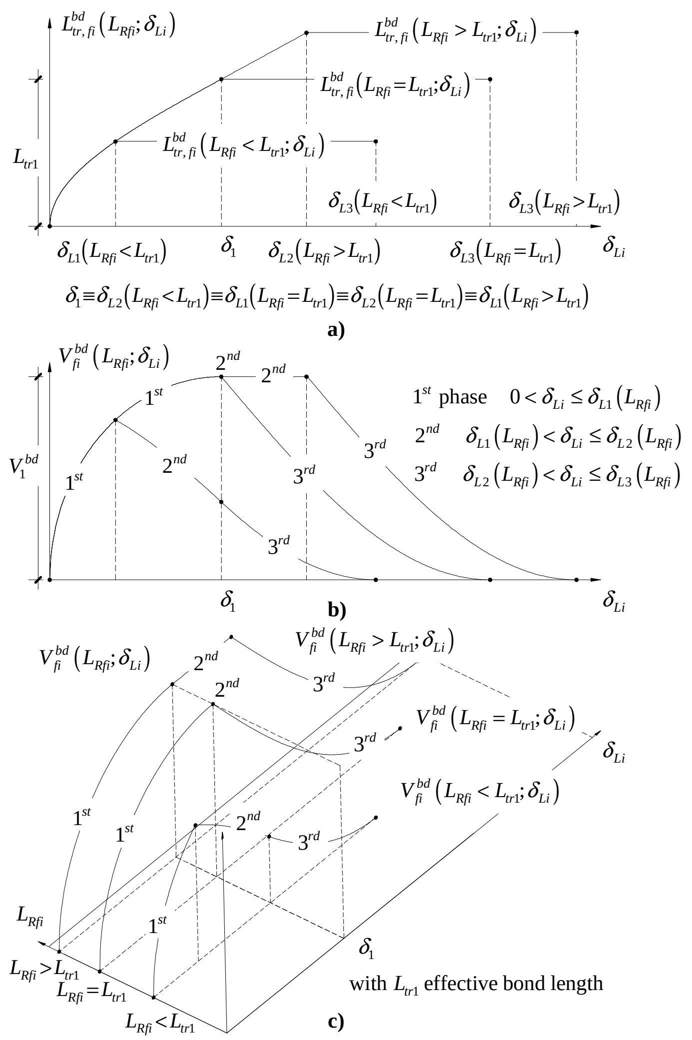


**Figure 3 —** Bond-based constitutive law of a single NSM FRP strip: (a) relationship between bond transfer length $L_{tr,fi}^{bd}\left(\delta_{Li};L_{Rfi}\right)$ and imposed end slip $\delta_{Li}$ for different values of resisting bond length $L_{Rfi}$; (b) bi-dimensional and (c) three-dimensional

representation of the relationship between force transferrable by bond $V_{fi}^{bd}\left(\delta_{Li};L_{Rfi}\right)$ and $\delta_{Li}$ for different values of $L_{Rfi}$.

**Comprehensive constitutive law**

At the $t_n$ load step, an iterative procedure ($q_m : q_1 \rightarrow q_e$) is carried out in order to determine the equilibrium condition ($q_e$) in the surrounding concrete depending on the current value of both imposed end slip $\delta_{Li}(t_n)$ and resisting bond length $L_{Rfi}(t_n;q_m)$ (Fig. 4). In particular, at the $q_m$ iteration of the $t_n$ load step, based on $L_{Rfi}(t_n;q_m)$ and $\delta_{Li}(t_n)$, the bond transfer length $L_{tr,fi}^{bd}\left[L_{Rfi}(t_n;q_m);\delta_{Li}(t_n)\right]$ and the corresponding bond-transferred force $V_{fi}^{bd}\left[L_{Rfi}(t_n;q_m);\delta_{Li}(t_n)\right]$ are evaluated as reported in Eq. (6) and Eq. (7), respectively. Then, the current value of the total transfer length is evaluated as follows:

$$L_{tr,fi}(t_n;q_m) = L_{fi}^{c}(t_{n-1};q_e) + L_{tr,fi}^{bd}\left[L_{Rfi}(t_n;q_m);\delta_{Li}(t_n)\right] + \Delta L_{fi}^{c}(t_n;q_m) \tag{17}$$

where $L_{fi}^{c}(t_{n-1};q_e)$ is the cumulative depth of the concrete fracture surface resulting from the equilibrium of the preceding $t_{n-1}$ load step and $\Delta L_{fi}^{c}(t_n;q_m)$ is the increment of concrete fracture depth corresponding to the current $t_n$, accumulated up to the current $q_m$ (Fig. 4):

$$\Delta L_{fi}^{c}(t_n;q_m) = \sum_{q_1}^{q_{m-1}} L_{tr,fi}^{bd}\left[L_{Rfi}(t_n;q_m);\delta_{Li}(t_n)\right] \tag{18}$$

Then, after having evaluated the concrete fracture capacity $V_{fi}^{cf}\left(L_{tr,fi}\right)$ as indicated in Eq. (16), if it is:

$$V_{fi}^{bd}\left[L_{Rfi}(t_n;q_m);\delta_{Li}(t_n)\right] \geq V_{fi}^{cf}\left[L_{tr,fi}(t_n;q_m)\right] \tag{19}$$

meaning that the surrounding concrete is not capable to carry the bond-transferred force, then it fractures and the bond transfer mechanism leaps forwards towards the free end. Thus, the parameters $L_{Rfi}(t_n;q_{m+1})$ and $\Delta L_{fi}^{c}(t_n;q_{m+1})$ are updated ($L_{Rfi}(t_n;q_{m+1}) = L_{Rfi}(t_n;q_m) - L_{tr,fi}^{bd}\left[L_{Rfi}(t_n;q_m);\delta_{Li}(t_n)\right]$, $\Delta L_{fi}^{c}(t_n;q_{m+1}) = \Delta L_{fi}^{c}(t_n;q_m) + L_{tr,fi}^{bd}\left[L_{Rfi}(t_n;q_m);\delta_{Li}(t_n)\right]$) and iteration is performed ($q_{m+1}$) (Fig. 4). At each of those leaps, the point representative of the strip state moves from one bond-based constitutive law $V_{fi}^{bd}\left[L_{Rfi}(t_n;q_m);\delta_{Li}\right]$ to the other $V_{fi}^{bd}\left[L_{Rfi}(t_n;q_{m+1});\delta_{Li}\right]$ and, as long as the updated value of $L_{Rfi}$ is larger or equal to the necessary bond transfer length $L_{tr}^{bd}[\delta_{Li}(t_n)]$, such leap is only visible in a three dimensional representation (Fig. 4). The necessary bond transfer length $L_{tr}^{bd}[\delta_{Li}(t_n)]$ is the bond transfer length that would be necessary, if $L_{Rfi}$ were infinite, to transmit the corresponding force to the surrounding concrete, with $L_{tr}^{bd}[\delta_{Li}(t_n)] = L_{tr}^{sf}[\delta_{Li}(t_n)]$ for $\delta_{Li}(t_n) \leq \delta_1$ and $L_{tr}^{bd}[\delta_{Li}(t_n)] = L_{tr1} + L_{tr}^{fs}[\delta_{Li}(t_n)]$ for $\delta_{Li}(t_n) > \delta_1$ (Fig. 4). Note also that, at each $q_m$ iteration, the equality $L_{Rfi}(t_n;q_m)+L^c_{fi}(t_{n-1};q_e)+\Delta L^c_{fi}(t_n;q_m)=L_{Rfi}(t_1;q_1)=\bar{L}_{fi}$ has to be fulfilled (Fig. 4c).

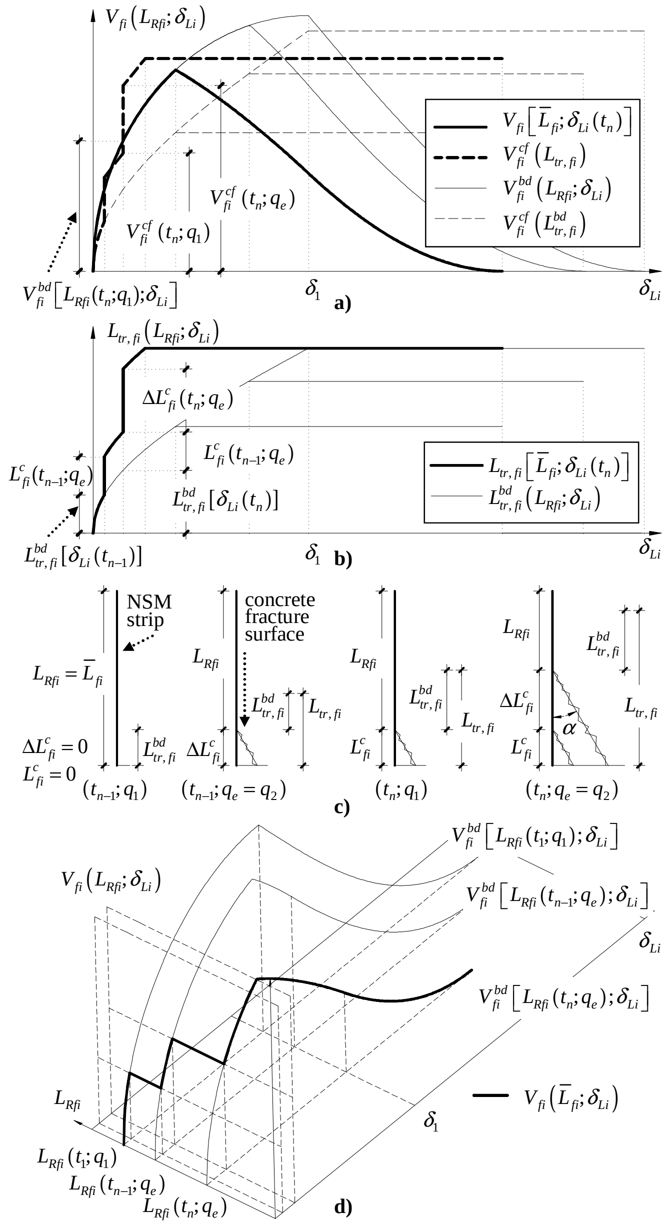


**Figure 4 —** Single NSM FRP strip comprehensive constitutive law in case in which concrete fracture remains shallow: a) resulting constitutive law $V_{fi}\left(\bar{L}_{fi};\delta_{Li}\right)$ in a bi-dimensional representation, b) resulting overall transfer length $L_{tr,fi}\left(\bar{L}_{fi};\delta_{Li}\right)$, c) section of the concrete prism and occurrence of subsequent fractures and d) resulting

constitutive law $V_{fi}\left(\bar{L}_{fi};\delta_{Li}\right)$ in a three-dimensional representation. Note that this plot has been done for an initial resisting bond length equal to the effective bond length.

More in detail, at the $q_m$ iteration of the $t_n$ load step, if concrete is not in equilibrium ($c_e = 0$), one of the following alternatives might occur:

- concrete fracture was deep ($d_f = 1$) but it did not reach the free end, *i.e.* the updated resisting bond length $L_{Rfi}(t_n; q_{m+1})$ is not long enough to mobilize, for the current $\delta_{Li}(t_n)$, a bond transfer length as large as the necessary one: $L_{Rfi} < L_{tr}^{bd}[\delta_{Li}(t_n)]$. Note that in this case, the passage of the point representative of the strip state from one bond-based constitutive law to the other is also visible in a bi-dimensional representation. Further details can be found elsewhere (Bianco 2008);
- concrete fracture was deep ($d_f = 1$) and it reached the free end, *i.e.* the updated resisting bond length $L_{Rfi}(t_n; q_{m+1})$ is null. Note is taken of the current value of the imposed end slip ($\delta_{Lu} \leftarrow \delta_{Li}(t_n)$) and the incremental procedure is terminated since a decision about the comprehensive constitutive law can already be taken ($u = 1$) (Fig. 5a).

On the contrary, if at the $q_m$ iteration of the $t_n$ load step, concrete is in equilibrium ($c_e = 1$), it is not necessary to iterate and one of the following alternatives might occur:

- the current value of bond-transferred force is larger or equal to the strip tensile rupture capacity ($V_{fi}^{bd} \geq V_f^{tr}$). The incremental procedure is terminated since, even if the surrounding concrete is in equilibrium, the strip has ruptured ($u = 2$) and note is taken of the ultimate imposed end slip ($\delta_{Lu} \leftarrow \delta_{Li}(t_n)$);
- the next value of the imposed end slip $\delta_{Li}(t_{n+1})$ is larger or equal to the one in correspondence of which the peak bond force is attained for the current value of the resisting bond length $\delta_{Li}(t_{n+1}) \geq \delta_{L1}\left[L_{Rfi}(t_n; q_e)\right]$. Since $V_{fi}^{bd}$ starts to decrease for $\delta_{Li}(t_{n+1})$, the incremental procedure is terminated and note is taken of the current value of the resisting bond length ($L_{Rfu} \leftarrow L_{Rfi}$) and of its relationship with the effective bond length $L_{tr1}$ ($u \leftarrow 3$ if $L_{Rfu} < L_{tr1}$, $u \leftarrow 4$ if $L_{Rfu} = L_{tr1}$ or $u \leftarrow 5$ if $L_{Rfu} > L_{tr1}$).
- concrete fracture was deep ($d_f = 1$) and it did not reach the free extremity. The incremental procedure is terminated ($u = 6$) (Fig. 5d);
- the next value of the imposed end slip $\delta_{Li}(t_{n+1})$ is smaller than the one where the peak bond force is attained for the current value of the resisting bond length $\delta_{Li}(t_{n+1}) < \delta_{L1}\left[L_{Rfi}(t_n; q_e)\right]$. Then, the imposed end slip is incremented and the iteration carried out.

The incremental procedure described above is terminated and, depending on the phenomenon characterizing the specific case at hand and the type of constitutive law associated ($u$), the parameters necessary to define $V_{fi}\left(\bar{L}_{fi};\delta_{Li}\right)$ are returned, *i.e.*:

- deep concrete fracture that reaches the strip's free extremity ($u=1$) or tensile rupture of the strip ($u=2$). The parameter necessary to determine the constitutive law is the imposed end slip $\delta_{Lu}$ in correspondence of which the peak of $V_{fi}\left(\bar{L}_{fi};\delta_{Li}\right)$ occurs. $V_{fi}\left(\bar{L}_{fi};\delta_{Li}\right)$ is given by the first bond phase of Eq. (7) for $0.0 \le \delta_{Li} \le \delta_{Lu}$ (Fig. 5a);
- shallow or absent concrete fracture with an ultimate value of resisting bond length smaller ($u=3$), equal ($u=4$) or larger ($u=5$) than the effective bond length. The parameter necessary to determine the comprehensive constitutive law is the ultimate value assumed by the resisting bond length $L_{Rfu}$. $V_{fi}\left(\bar{L}_{fi};\delta_{Li}\right)$ is given by Eq. (7) for $L_{Rfi}=L_{Rfu}$ (Fig. 5b-c);
- deep tensile fracture with an ultimate value of resisting bond length very short but not null ($u=6$). The parameters necessary to determine the comprehensive constitutive law are both the imposed end slip $\delta_{Lu}$ in correspondence of which the peak of $V_{fi}\left(\bar{L}_{fi};\delta_{Li}\right)$ occurs and the ultimate value assumed by the resisting bond length $L_{Rfu}$. $V_{fi}\left(\bar{L}_{fi};\delta_{Li}\right)$ is given by: the first bond phase of Eq. (7) for $0.0 \le \delta_{Li} \le \delta_{Lu}$, the second bond phase of Eq. (7) for $\delta_{Lu} < \delta_{Li} \le \delta_{L2}\left(L_{Rfu}\right)$ and the third bond phase of Eq. (7) for $\delta_{L2}\left(L_{Rfu}\right) < \delta_{Li} \le \delta_{L3}\left(L_{Rfu}\right)$ (Fig. 5d).

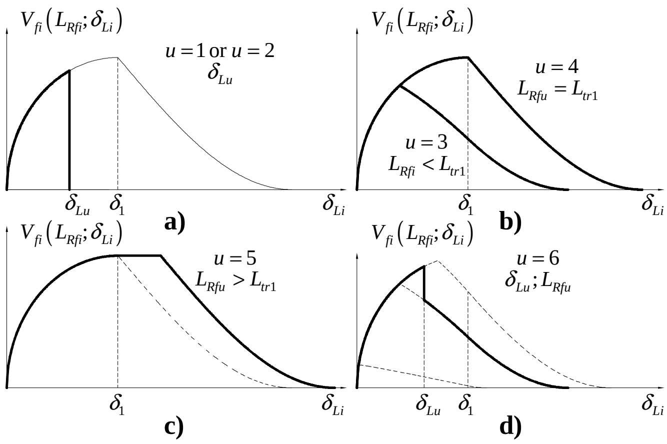


**Figure 5 —** Possible comprehensive constitutive law of a NSM FRP strip confined to a prism of concrete: (a) concrete that reaches the free extremity ($u=1$) or strip tensile rupture ($u=2$), superficial and/or absent concrete fracture and ultimate resisting bond length (b) smaller ($u=3$) or equal ($u=4$) or (c) larger ($u=5$) than the effective bond length and (d) deep concrete fracture ($u=6$).

**MAXIMUM EFFECTIVE CAPACITY OF A SINGLE NSM FRP STRIP**

The effective capacity $V_{fi,eff}(\gamma)$ is the average of the NSM FRP strip capacity along the CDC $V_{fi,CDC}(\gamma;\xi)$ for a given value of the CDC opening angle $\gamma$ (*e.g.* Fig. 6), where $\xi$ is the reference system assumed along the CDC (Fig. 1a). $V_{fi,CDC}(\gamma;\xi)$ is obtained by introducing the kinematic compatibility ($\delta_{Li}(\gamma;\xi)=\frac{1}{2}\cdot\xi\cdot\gamma\cdot\sin(\theta+\beta)$) into the comprehensive constitutive law of the single average-available-bond-length NSM FRP strip $V_{fi}\left(\bar{L}_f;\delta_{Li}\right)$. For the sake of brevity, all of the details are herein omitted but they can be found elsewhere (Bianco 2008). The equation to evaluate the maximum effective capacity $V_{fi,eff}^{\max}$ and the value of the CDC opening angle $\gamma_{\max}$ in correspondence of which it is attained, assume different features as function of the type ($u$) of the comprehensive constitutive law characterizing the specific case at hand.

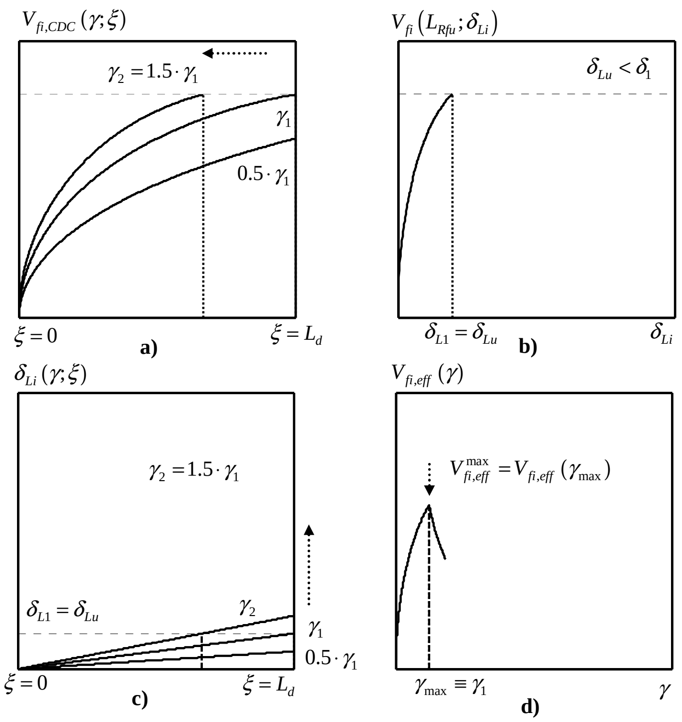


**Figure 6 —** Maximum effective capacity along the CDC for the cases of concrete fracture that reaches the strip's free extremity ($u=1$) or strip's tensile rupture ($u=2$): a) capacity $V_{fi,CDC}(\gamma;\xi)$ and c) imposed end slip $\delta_{Li,CDC}(\gamma;\xi)$ distribution along the CDC for different values of the CDC opening angle $\gamma$, b) comprehensive constitutive law and d) effective capacity as function of the CDC opening angle $\gamma$.

**<u>Cases of concrete fracture that reaches the strip's free extremity (u = 1) or strip tensile rupture (u = 2)</u>**

In these cases, the exact value of the maximum effective capacity is attained for a value of the CDC opening angle $\gamma$ such as to yield an imposed end slip at the end of the crack ( $\delta_{Li}(L_d)$ ), equal to $\delta_{Lu}$ (Fig. 6) *i.e.*:

$$V_{fi,eff}^{\max}=V_{fi,eff}(\gamma_{\max})=\frac{1}{L_d}\cdot\left\{A_1\cdot C_1^{sf}\cdot L_d^2\cdot\gamma_{\max}+\frac{A_2\cdot C_2^{sf}}{2\cdot A_3\cdot\gamma_{\max}}\cdot\right.$$
$$\left.\cdot\left[\arcsin(1-A_3\cdot\gamma_{\max}\cdot L_d)+(1-A_3\cdot\gamma_{\max}\cdot L_d)\cdot\sqrt{1-(1-A_3\cdot\gamma_{\max}\cdot L_d)^2}-\frac{\pi}{2}\right]\right\} \tag{20}$$

where:

$$A_1=-\frac{L_p\cdot J_3\cdot\lambda^3\cdot\sin(\theta+\beta)}{4\cdot\tau_0\cdot J_1};\ A_2=L_p\cdot J_3\cdot\lambda;\ A_3=\frac{\lambda^2\cdot\sin(\theta+\beta)}{2\cdot\tau_0\cdot J_1} \tag{21}$$

are integration constants independent of the type ($u$) of comprehensive constitutive law and:

$$\gamma_{\max}=\gamma_1=\frac{2\cdot\delta_{Lu}}{L_d\cdot\sin(\theta+\beta)} \tag{22}$$

**<u>Case of shallow concrete fracture and strip ultimate resisting bond length smaller than the effective bond length (u = 3)</u>**

In this case, the maximum effective capacity is attained for a value of $\gamma$ very close to $\gamma_2$ that is the value of the CDC opening angle such as to yield an imposed end slip at the end of the crack, equal to $\delta_{L2}\left(L_{Rfu}\right)$. For the sake of simplicity, it is assumed that $V_{fi}^{\max}$ is effectively attained for $\gamma_2$ accepting a slight approximation (Bianco 2008) *i.e.*:

$$V_{fi,eff}^{\max}=\frac{1}{L_d}\cdot\left\{\left[A_1\cdot\left(C_1^{sf}-C_1\right)\cdot\left(\frac{2\cdot\delta_{L1}}{\sin(\theta+\beta)}\right)^2+\left(C_2^{sf}+C_2\right)\cdot\frac{A_2\cdot\Phi_1(\delta_{L1})}{2\cdot A_3}-\right.\right.$$
$$\left.-\frac{A_2\cdot C_2^{sf}\cdot\pi}{4\cdot A_3}-\frac{2\cdot A_2\cdot C_1\cdot\delta_{L1}}{\sin(\theta+\beta)}\right]\cdot\frac{1}{\gamma_{\max}}-\frac{A_2\cdot C_2}{2\cdot A_3\cdot\gamma_{\max}}\cdot\left[\arcsin(1-A_3\cdot\gamma_{\max}\cdot L_d)\ +\right. \tag{23}$$
$$\left.\left.+(1-A_3\cdot\gamma_{\max}\cdot L_d)\cdot\sqrt{1-(1-A_3\cdot\gamma_{\max}\cdot L_d)^2}\right]+A_2\cdot C_1\cdot L_d+A_1\cdot C_1\cdot\gamma_{\max}\cdot L_d^2\right\}$$

where $A_1$, $A_2$ and $A_3$ are given by Eq. (21), $\delta_{L1}=\delta_{L1}\left(L_{Rfu}\right)$ by Eq. (13) and:

$$C_1\left(L_{Rfu}\right)=C_1^{sf}-C_1^{sf}\cdot\cos\left(\lambda\cdot L_{Rfu}\right)-C_2^{sf}\cdot\sin\left(\lambda\cdot L_{Rfu}\right)$$
$$C_2\left(L_{Rfu}\right)=-C_2^{sf}-C_1^{sf}\cdot\sin\left(\lambda\cdot L_{Rfu}\right)+C_2^{sf}\cdot\cos\left(\lambda\cdot L_{Rfu}\right) \tag{24}$$

$$\Phi_1(\delta_{Li})=\arcsin\left(1-\frac{2\cdot A_3\cdot\delta_{Li}}{\sin(\theta+\beta)}\right)+\left(1-\frac{2\cdot A_3\cdot\delta_{Li}}{\sin(\theta+\beta)}\right)\cdot\sqrt{1-\left(1-\frac{2\cdot A_3\cdot\delta_{Li}}{\sin(\theta+\beta)}\right)^2} \tag{25}$$

$$\gamma_{\max}=\gamma_2=\frac{2\cdot\delta_{L2}\left(L_{Rfu}\right)}{L_d\cdot\sin(\theta+\beta)} \tag{26}$$

**<u>Case of shallow concrete fracture and strip's ultimate resisting bond length equal to the effective bond length (u = 4)</u>**

In this case, the maximum effective capacity is attained for a value of the CDC opening angle $\gamma$ slightly larger than $\gamma_1 = 2 \cdot \delta_1 / (L_d \cdot \sin(\theta+\beta))$ at which the $\delta_1$ end slip occurs at the end of the CDC (Bianco 2008). Anyway, since the expressions of $V_{fi,eff}(\gamma)$ are very complex for $\gamma_1 < \gamma \leq \gamma_2$, instead of carrying out the derivative ($dV_{fi,eff}(\gamma)/d\gamma = 0$) to search for the exact value of $\gamma_{\max}$, it is deemed reasonable to assume $\gamma_1$ as angle where the maximum effective capacity occurs. The solution so obtained, slightly underestimating the real maximum, is:

$$V_{fi,eff}^{\max} = \frac{1}{L_d} \cdot \left\{ A_1 \cdot C_1^{sf} \cdot L_d^2 \cdot \gamma_{\max} + \frac{A_2 \cdot C_2^{sf}}{2 \cdot A_3 \cdot \gamma_{\max}} \cdot \left[ \arcsin(1 - A_3 \cdot \gamma_{\max} \cdot L_d) + (1 - A_3 \cdot \gamma_{\max} \cdot L_d) \cdot \sqrt{1 - (1 - A_3 \cdot \gamma_{\max} \cdot L_d)^2} - \frac{\pi}{2} \right] \right\} \tag{27}$$

where $A_1$, $A_2$ and $A_3$ are given by Eq. (21) and:

$$\gamma_{\max} = \gamma_1 = \frac{2 \cdot \delta_1}{L_d \cdot \sin(\theta+\beta)} \tag{28}$$

**Case of shallow concrete fracture and strip's ultimate resisting bond length larger than the effective bond length (u = 5)**

In this case, the maximum effective capacity is attained for a value of the CDC opening angle $\gamma$ slightly larger than $\gamma_2 = 2 \cdot \delta_{L2} / (L_d \cdot \sin(\theta+\beta))$ at which the end slip $\delta_{L2}(L_{Rfu})$ occurs at the end of the CDC (Bianco 2008). Again, since the expressions of $V_{fi,eff}(\gamma)$ are very complex for $\gamma_2 < \gamma \leq \gamma_3$, it is deemed a reasonable compromise between accuracy of prediction and computational demand, to assume $\gamma_2$ as angle in correspondence of which the maximum effective capacity occurs. The solution so obtained, slightly underestimating the real maximum, is:

$$V_{fi,eff}^{\max} = \frac{1}{L_d} \cdot \left\{ \left[ A_1 \cdot C_1^{sf} \cdot \left( \frac{2 \cdot \delta_1}{\sin(\theta+\beta)} \right)^2 + \frac{C_2^{sf} \cdot A_2 \cdot \Phi_1(\delta_1)}{2 \cdot A_3} - \frac{A_2 \cdot C_2^{sf} \cdot \pi}{4 \cdot A_3} \right] \cdot \frac{1}{\gamma_{\max}} + V_{f1}^{bd} \cdot \left( L_d - \frac{2 \cdot \delta_1}{\gamma_{\max} \cdot \sin(\theta+\beta)} \right) \right\} \tag{29}$$

where $A_1$, $A_2$ and $A_3$ are given by Eq. (21), $\Phi_1(\delta_1)$ as given by Eq. (25) and:

$$\gamma_{\max} = \gamma_2 = \frac{2 \cdot \delta_{L2}(L_{Rfu})}{L_d \cdot \sin(\theta+\beta)} \tag{30}$$

**Case of deep concrete fracture (u = 6)**

In this case, it is not possible to tell *a priori* if the maximum effective capacity is attained at a value of the CDC opening angle such as to yield an imposed end slip at the end of the crack, equal to $\delta_{Lu}$ or to $\delta_{L2}(L_{Rfu})$ (Bianco 2008). Thus, the maximum effective capacity will be given by:

$$V_{fi,eff}^{\max} = \max\left\{ V_{fi,eff}^{\max 1}; V_{fi,eff}^{\max 2} \right\} \tag{31}$$

where:

$$V_{fi,eff}^{\max 1} = V_{fi,eff}(\gamma_{\max 1}) = \frac{1}{L_d} \cdot \left\{ A_1 \cdot C_1^{sf} \cdot L_d^2 \cdot \gamma_{\max 1} + \frac{A_2 \cdot C_2^{sf}}{2 \cdot A_3 \cdot \gamma_{\max 1}} \cdot \right.$$
$$\left. \cdot \left[ \arcsin(1 - A_3 \cdot \gamma_{\max 1} \cdot L_d) + (1 - A_3 \cdot \gamma_{\max 1} \cdot L_d) \cdot \sqrt{1 - (1 - A_3 \cdot \gamma_{\max 1} \cdot L_d)^2} - \frac{\pi}{2} \right] \right\} \tag{32}$$

$$\gamma_{\max 1} = \gamma_1 = \frac{2 \cdot \delta_{Lu}}{L_d \cdot \sin(\theta + \beta)} \tag{33}$$

and:

$$V_{fi,eff}^{\max 2} = V_{fi,eff}(\gamma_{\max 2}) =$$
$$\frac{1}{L_d} \cdot \left\{ \left[ A_1 \cdot \left(C_1^{sf} - C_1\right) \cdot \left( \frac{2 \cdot \delta_{Lu}}{\sin(\theta + \beta)} \right)^2 + \left(C_2^{sf} + C_2\right) \cdot \frac{A_2 \cdot \Phi_1(\delta_{Lu})}{2 \cdot A_3} - \frac{A_2 \cdot C_2^{sf} \cdot \pi}{4 \cdot A_3} + \right. \right.$$
$$\left. - \frac{2 \cdot A_2 \cdot C_1 \cdot \delta_{Lu}}{\sin(\theta + \beta)} \right] \cdot \frac{1}{\gamma_{\max 2}} + - \frac{A_2 \cdot C_2}{2 \cdot A_3 \cdot \gamma_{\max 2}} \cdot \left[ \arcsin(1 - A_3 \cdot \gamma_{\max 2} \cdot L_d) \; + \right. \tag{34}$$
$$\left. \left. + (1 - A_3 \cdot \gamma_{\max 2} \cdot L_d) \cdot \sqrt{1 - (1 - A_3 \cdot \gamma_{\max 2} \cdot L_d)^2} \right] + A_2 \cdot C_1 \cdot L_d + A_1 \cdot C_1 \cdot \gamma_{\max 2} \cdot L_d^2 \right\}$$

$$\gamma_{\max 2} = \gamma_2 = \frac{2 \cdot \delta_{L2}\left(L_{Rfu}\right)}{L_d \cdot \sin(\theta + \beta)} \tag{35}$$

and where $A_1$, $A_2$ and $A_3$ are given by Eq. (21), $C_1\left(L_{Rfu}\right)$ and $C_2\left(L_{Rfu}\right)$ as given by Eq. (24) and $\Phi_1(\delta_{Lu})$ as given by Eq. (25).

## ACTUAL AND DESIGN VALUE OF THE SHEAR STRENGTHENING CONTRIBUTION

The actual $V_f$ and design value $V_{fd}$ of the NSM shear strength contribution, can be obtained as follows:

$$V_{fd} = \frac{1}{\gamma_{Rd}} \cdot V_f = \frac{1}{\gamma_{Rd}} \cdot \left( 2 \cdot N_{f,\text{int}}^{l} \cdot V_{fi,eff}^{\max} \cdot \sin\beta \right) \tag{36}$$

where $\gamma_{Rd}$ is the partial safety factor, divisor of a capacity, that can be assumed as 1.1-1.2 according to the level of uncertainty affecting the input parameters but, in this respect, a reliability-based calibration is needed.

## MODEL APPRAISAL

The proposed model was herein applied to the T cross-section RC beams tested by Dias and Barros (2008). The beams tested were RC beams characterized by the same test set-up with the same ratio between the shear span and the beam effective depth ($a/d = 2.5$), the same amount of longitudinal reinforcement, the same kind of CFRP strips and epoxy adhesive. The details of the beams taken to appraise the predictive performance of the developed model are listed in Table 1. Those beams are characterized by the following common geometrical and mechanical parameters: $b_w = 180\ mm$; $h_w = 300\ mm$; $f_{fu} = 2952\ MPa$; $f_{cm} = 31.11\ MPa$; $E_f = 166.6\ GPa$; $a_f = 1.4\ mm$; $b_f = 10.0\ mm$ (1 *mm* = 0.0394 *in* - 1 *N* = 0.2248 *lb* - 1000 *psi* = 6.9 *MPa*). The CDC inclination angle $\theta$ adopted in the simulations, listed in Table 1 for all the beams analyzed, is the one experimentally observed by inspecting the crack patterns. The angle $\alpha$ was assumed equal to 28.5°, being the average of values obtained in a previous investigation (Bianco *et al.* 2006) by back analysis of experimental data. The parameter characterizing the loading process is: $\dot{\delta}_{Li} = 0.0001\, rads$, which guarantees a good compromise between accuracy of prediction and computational demand. Concrete average tensile strength $f_{ctm}$ was calculated from the average compressive strength by means of the formulae of the CEB Fib Model Code 1990 resulting in 2.45 *MPa*.

The parameters characterizing the adopted local bond stress-slip relationship (Fig. 1b) are: $\tau_0 = 20.1\, MPa$ and $\delta_1 = 7.12\, mm$ (Bianco 2008). Those values were obtained by the values characterizing the more sophisticated local bond stress-slip relationship adopted in previous works (Bianco *et al.* 2009a, 2010), by fixing the value of $\tau_0 = 20.1\, MPa$ and determining $\delta_1 = 7.12\, mm$ by equating the fracture energy. In this respect, it has to be underlined that the necessity is felt to develop rigorous equations that would allow the values $(\tau_0, \delta_1)$ characterizing the local bond stress slip relationship to be determined on the basis of: a) superficial chemical and micro-mechanical properties of FRP, adhesive and concrete, and b) the adhesive layer thickness. Nonetheless, further research is, in this respect, required.

Table 1 shows that the model, in general, provides reasonable underestimates of the experimental recordings $V_f^{\exp}$ since the ratio $V_f / V_f^{\exp}$ presents mean value and standard deviation equal to 0.85 and 0.36, respectively. The values of NSM shear strength contribution have also been compared with the maximum values provided by the more refined model in correspondence of three different geometrical configurations that the occurred CDC could assume with respect to the strip ($V_{f,1}^{\max}$, $V_{f,2}^{\max}$ and $V_{f,3}^{\max}$ in Table 1). The simplified model herein presented, in some cases (*e.g.* beam 2S-5LV) provides a value of the NSM shear strength contribution that lies in between the minimum and maximum values obtained by the more refined model and in other cases (*e.g.* 2S-5LI45) that is rather lower than the lower bound of the values obtained by the more refined model. This is reasonable, since the approximations introduced inevitably reduce the accuracy.

**Table 1 —** Values of the parameters characterizing the beams adopted to appraise the formulation proposed (1 *mm* = 0.0394 *in* - 1 *N* = 0.2248 *lb* - 1000 *psi* = 6.9 *MPa*).

| Beam Label | $\theta^{\exp}$ ° | $\beta$ ° | $s_f$ *mm* | Steel Stirrups | $V_{f,1}^{\max}$ *kN* | $V_{f,2}^{\max}$ *kN* | $V_{f,3}^{\max}$ *kN* | $V_f^{\exp}$ *kN* | $\bar{L}_f$ *mm* | $u$ | $V_f$ *kN* |
|---|---|---|---|---|---|---|---|---|---|---|---|
| 2S-3LV | 40 | 90 | 267 | Φ6/300 | 18.53 | 6.46 | 55.33 | **22.20** | 75.96 | 3 | **10.77** |
| 2S-5LV | 40 | 90 | 160 | “ | 52.33 | 26.42 | 55.34 | **25.20** | 82.87 | 6 | **30.97** |
| 2S-8LV | 36 | 90 | 100 | “ | 68.58 | 58.88 | 64.33 | **48.60** | 77.34 | 3 | **29.59** |
| 2S-3LI45 | 45 | 45 | 367 | “ | 35.10 | 15.41 | 45.73 | **29.40** | 164.75 | 3 | **23.44** |
| 2S-5LI45 | 45 | 45 | 220 | “ | 46.11 | 49.14 | 45.74 | **41.40** | 134.35 | 3 | **23.19** |
| 2S-8LI45 | 36 | 45 | 138 | “ | 75.89 | 79.71 | 78.73 | **40.20*** | 106.73 | 6 | **59.55** |
| 2S-3LI60 | 33 | 60 | 325 | “ | 50.69 | 18.90 | 51.68 | **35.40** | 169.16 | 3 | **30.74** |
| 2S-5LI60 | 36 | 60 | 195 | “ | 36.37 | 36.59 | 48.55 | **46.20** | 77.27 | 6 | **22.27** |
| 2S-7LI60 | 33 | 60 | 139 | “ | 52.98 | 63.07 | 67.58 | **54.60** | 91.05 | 6 | **60.80** |

The model herein proposed, as the more refined one, both seem to provide reasonable estimates of the experimental recordings regardless of the amount of existing stirrups. Actually, the authors think that the amount of existing stirrups affects the depth to which the concrete fracture can penetrate the beam web core but, since it also affects the CDC inclination angle $\theta^{\exp}$, both models end up giving satisfactory results regardless of the amount of existing stirrups (Table 1). Anyway, in this respect, further research is needed.

## CONCLUSIONS

A closed-form design procedure to evaluate the NSM FRP strips shear strength contribution to RC beams was developed by simplifying a more sophisticated model recently developed. That procedure was obtained by introducing some substantial simplifications, such as: a) assuming a simplified local bond stress-slip relationship, b) taking into consideration the average-available-bond-length NSM FRP strip confined to a concrete prism, and c) assuming the concrete fracture surfaces as being semi-pyramidal instead of semi-conical. Given those simplifications, the procedure is based on the evaluation of the constitutive law of the average-available-bond-length strip and the determination of the maximum effective capacity that this latter can provide during the loading process of the strengthened beam, once the kinematic mechanism has been suitably imposed. The most complicate task is the correct evaluation of the single average-available-bond-length strip's comprehensive constitutive law, but it can be easily carried out by means of the informatics tools available to every structural engineer nowadays. The estimates of the NSM shear strength contribution obtained by means of that simplified model showed a reasonable agreement with both the experimental recordings and the predictions obtained by a more sophisticated model. Anyway, the introduction of substantial simplifications inevitably brought a loss of accuracy. Moreover, many aspects such as the correct evaluation of the local bond stress slip relationship and the issue of the interaction with existing stirrups still have to be addressed.

## ACKNOWLEDGEMENTS

The authors of the present work wish to acknowledge the support provided by the "Empreiteiros Casais", S&P®, degussa® Portugal, and Secil (Unibetão, Braga). The study reported in this paper forms a part of the research program "CUTINEMO - Carbon fiber laminates applied according to the near surface mounted technique to increase the flexural resistance to negative moments of continuous reinforced concrete structures" supported by FCT, PTDC/ECM/73099/2006. Also, this work was carried out under the auspices of the Italian DPC-ReLuis Project (repertory n. 540), Research Line 8, whose financial support is greatly appreciated.

## REFERENCES

Bianco, V., Barros, J.A.O., Monti, G., (2006). "Shear Strengthening of RC beams by means of NSM laminates: experimental evidence and predictive models", Technical report 06-DEC/E-18, Dep. Civil Eng., School Eng. University of Minho, Guimarães- Portugal.

Bianco, V., Barros, J.A.O., Monti, G., (2007). "Shear Strengthening of RC beams by means of NSM strips: a proposal for modeling debonding", Technical report 07-DEC/E-29, Dep. Civil Eng., School Eng. University of Minho, Guimarães- Portugal.

Bianco, V., (2008). “Shear Strengthening of RC beams by means of NSM FRP strips: experimental evidence and analytical modeling”, PhD Thesis, Dept. of Structural Engrg. and Geotechnics, Sapienza University of Rome, Italy, submitted on December 2008.

Bianco, V., Barros, J.A.O., Monti, G., (2009a). “Three dimensional mechanical model for simulating the NSM FRP strips shear strength contribution to RC beams”, Engineering Structures, 31(4), April 2009, 815-826.

Bianco, V., Barros, J.A.O., Monti, G., (2009b). “Bond Model of NSM FRP strips in the context of the Shear Strengthening of RC beams”, ASCE Journal of Structural Engineering, 135(6), June 2009.

Bianco, V., Barros, J.A.O., Monti, G., (2010). “New approach for modeling the contribution of NSM FRP strips for shear strengthening of RC beams”, ASCE Journal of Composites for Construction, 14(1), January/February 2010.

CEB-FIP Model Code 90, (1993) Bulletin d’Information N° 213/214, Final version printed by Th. Telford, London, (1993; ISBN 0-7277-1696-4; 460 pages).

Dias, S.J.E. and Barros, J.A.O., (2008). “Shear Strengthening of T Cross Section Reinforced Concrete Beams by Near Surface Mounted Technique”, Journal of Composites for Construction, ASCE, Vol. 12, No. 3, pp. 300-311.

Monti, G., Renzelli, M., Luciani, P., (2003) “FRP Adhesion to Uncracked and Cracked Concrete Zones”, Proceedings of the 6th International Symposium on Fibre-Reinforced Polymer (FRP) Reinforcement for Concrete Structures (FRPRCS-6), Singapore, July, 183-192.

Monti, G., Santinelli, F., Liotta, M.A., (2004) “Mechanics of FRP Shear Strengthening of RC beams”, Proc. ECCM 11, Rhodes, Greece.

Monti, G., Liotta, M.A., (2007) “Tests and design equations for FRP-strengthening in shear”, Construction and Building Materials (2006), 21(4), April 2007, 799-809.

Mohammed Ali, M.S., Oehlers, D.J., Seracino, R. (2006). “Vertical shear interaction model between external FRP transverse plates and internal stirrups”, Engineering Structures 28, 381-389.

Mohammed Ali, M.S., Oehlers, D.J., Griffith, M.C., Seracino, R. (2007). “Interfacial stress transfer of near surface-mounted FRP-to-concrete joints”, Engineering Structures 30, 1861-1868.

Rizzo, A. and De Lorenzis, L., (2009) “Behaviour and capacity of Rc beams strengthened in shear with NSM FRP reinforcement”, Construction and Building Materials, Vol. 3, n. 4, April 2009, 1555-1567.

Yuan, H., Teng, J.G., Seracino, R., Wu, Z.S., Yao, J. (2004). “Full-range behavior of FRP-to-concrete bonded joints”, Engineering Structures, 26, 553-565.